

Column design of cold-formed stainless steel slender circular hollow sections

Ben Young[†]

Department of Civil Engineering, The University of Hong Kong, Pokfulam Road, Hong Kong

Ehab Ellobody[‡]

Department of Structural Engineering, Faculty of Engineering, Tanta University, Tanta, Egypt

(Received May 23, 2005, Accepted October 25, 2005)

Abstract. This paper describes the design and behaviour of cold-formed stainless steel slender circular hollow section columns. The columns were compressed between fixed ends at different column lengths. The investigation focused on large diameter-to-plate thickness (D/t) ratio ranged from 100 to 200. An accurate finite element model has been developed. The initial local and overall geometric imperfections have been incorporated in the model. The column strengths, load-shortening curves as well as failure modes were predicted using the finite element model. The nonlinear finite element model was verified against test results. An extensive parametric study was carried out to study the effects of cross-section geometries on the strength and behaviour of stainless steel slender circular hollow section columns with large D/t ratio. The column strengths predicted from the parametric study were compared with the design strengths calculated using the American Specification, Australian/New Zealand Standard and European Code for cold-formed stainless steel structures. It is shown that the design strengths obtained using the Australian/New Zealand and European specifications are generally unconservative for the cold-formed stainless steel slender circular hollow section columns, while the American Specification is generally quite conservative. Therefore, design equation was proposed in this study.

Keywords: cold-formed; columns; circular hollow sections; finite element; modeling; slender sections; stainless steel; structural design.

1. Introduction

In recent years, stainless steel structural members have been commonly used due to its high corrosion resistance, ease of construction and maintenance as well as aesthetic appearance. Tests of cold-formed stainless steel columns were conducted by Rasmussen and Hancock (1993), Talja and Salmi (1995), Rasmussen (2000), Macdonald *et al.* (2000), Gardner (2002), Young and Liu (2003) and Young and Lui (2005). These investigations focused on square and rectangular hollow sections as well as channel sections. There are not many research being reported on cold-formed stainless steel circular hollow

[†]Associate Professor, Corresponding author, E-mail: young@hku.hk

[‡]Lecturer, E-mail: ehab_ellobody@tanta.edu.eg

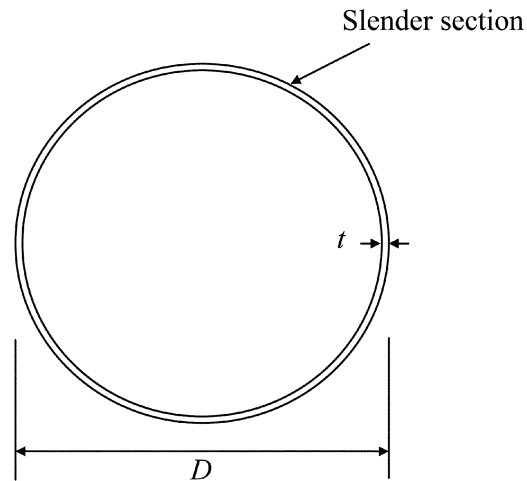


Fig. 1 Definition of symbols for stainless steel slender circular hollow section

section columns. Young and Hartono (2002) conducted a series of tests on cold-formed stainless steel circular hollow section columns.

Local buckling is a major consideration in the design of slender sections. Local buckling and shift of effective centroid of cold-formed steel columns have been investigated by Young and Rasmussen (1999), and Young (2005). The experimental local buckling loads were compared with the theoretical local buckling loads obtained using an elastic finite strip buckling analysis. Jiao and Zhao (2003) investigated the behaviour of very high strength carbon steel circular tubes. However, investigation on cold-formed stainless steel slender circular hollow section columns is rarely found in the literature. Gardner and Nethercot (2004) described numerical modeling of stainless steel hollow sections using ABAQUS program. Ellobody and Young (2005) developed a numerical model for fixed-ended cold-formed high strength stainless steel square and rectangular hollow section columns using ABAQUS (2004) program.

The purpose of this paper is to investigate the behaviour of cold-formed stainless steel slender circular hollow section columns with large diameter-to-plate thickness (D/t) ratio, where local buckling is a major consideration in the design. The columns had large D/t ratio ranged from 100 to 200, as shown in Fig. 1. The finite element program ABAQUS (2004) was used in the analysis. The numerical results were verified against the test results. Parametric study was performed to investigate the effect of local buckling on the design and behaviour of cold-formed stainless steel slender circular hollow section columns with large D/t ratio. Effective area equation was proposed to evaluate the axial strength of cold-formed stainless steel slender circular hollow section columns.

2. Summary of experimental investigation

2.1. General

A test program on cold-formed stainless steel circular hollow section columns performed by Young and Hartono (2002) provided the experimental ultimate loads and load-shortening curves of columns

compressed between fixed ends. Three series (Series C1, C2 and C3) of circular hollow section columns were tested. The test specimens were cold-rolled from annealed flat strips of type 304 stainless steel. Each specimen was cut to a specified length (L) ranging from 550 to 3000 mm. The measured cross-section dimensions of the test specimens are detailed in Young and Hartono (2002). The Series C1, C2 and C3 had an average measured outer diameter (D) of 89.0, 168.7, and 322.8 mm and an average thickness (t) of 2.78, 3.34 and 4.32 mm, respectively. The average measured outer diameter-to-thickness (D/t) ratio is 32.0, 50.5 and 74.7 for Series C1, C2 and C3, respectively. The test specimens are labeled such that the test series and specimen length could be identified from the label. For example, the label "C1L1000" defines the specimen belonged to test Series C1, and the letter "L" indicates the length of the specimen followed by the nominal column length of the specimen in mm (1000 mm).

The material properties of each series of specimens were determined by tensile coupon tests. The coupons were taken from the untested specimens at 90° from the weld in the longitudinal direction. The coupon dimensions and the tests conformed to the Australian Standard AS 1391 (1991) for the tensile testing of metals using 12.5 mm wide coupons of gauge length 50 mm. The Young's modulus (E_o) was measured as 188, 200 and 203 GPa as well as the measured static 0.2% proof stress ($\sigma_{0.2}$) was 268, 285 and 255 MPa for Series C1, C2 and C3, respectively. The measured elongation after fracture based on a gauge length of 50 mm was 58, 56 and 62% for Series C1, C2 and C3, respectively. The Ramberg-Osgood parameter (n) that describes the shape of the stress-strain curve (Ramberg and Osgood 1943) was 4, 7 and 5 for Series C1, C2 and C3, respectively. The tensile coupon tests are detailed in Young and Hartono (2002). The initial overall geometric imperfections of the specimens were measured prior to testing. The average values of overall imperfections at mid-length were 1/1715, 1/3778 and 1/3834 of the specimen length for Series C1, C2 and C3, respectively. The measured overall geometric imperfections for each test specimen are detailed in Young and Hartono (2002). The initial local geometric imperfections of the tested cold-formed stainless steel circular hollow section columns were not reported by Young and Hartono (2002). However, the values of the initial geometric imperfections

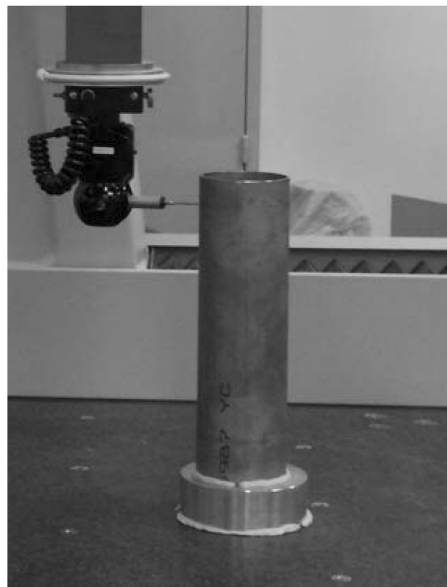


Fig. 2 Mitutoyo co-ordinate measuring machine for local imperfection measurements

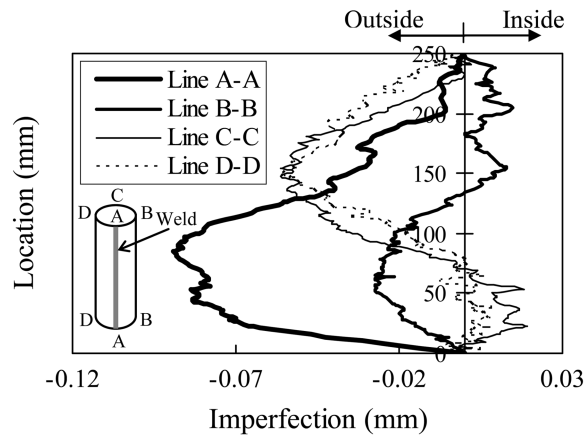


Fig. 3 Measured local geometric imperfection profiles for Series C1 specimen of 250 mm in length

are important for finite element analysis. Hence, the initial local geometric imperfections of the stainless steel circular hollow section specimen belonging to the same batch as the column test specimens are measured in this study and reported in this paper.

2.2. Measurements of initial local geometric imperfections

Measurements of initial local imperfections are carried out in this study by using the Coordinate Measuring Machine (CMM) as shown in Fig. 2. The CMM machine uses the standard touch probe for inspection and measurement of any objects. It can also employ a laser scanner to trace the profile of three-dimensional objects. A cold-formed stainless steel circular hollow section test specimen of 250 mm in length of Series C1 was used for the measurement of local imperfections. An automatic feed was used to rotate the touch probe indicator around the specimen. The measurements were taken at the longitudinal quarter lines A-A (at weld position), B-B, C-C and D-D of the specimen as shown in Fig. 3. Readings were taken at regular intervals of 2 mm and the maximum magnitude of local plate imperfection was 0.089 mm, which is equal to 3.2% of the plate thickness of the specimen belonged to Series C1. Fig. 3 shows the measured initial local geometric imperfection profiles of the specimen. The same factor was used to predict the initial local geometric imperfections for Series C2 and C3.

3. Numerical investigation

3.1. General

The finite element program ABAQUS (2004) was used to investigate the buckling behaviour of cold-formed stainless steel slender circular hollow section columns. The tests conducted by Young and Hartono (2002) were modeled using the measured geometry, initial local and overall geometric imperfections and material properties. Finite element analysis for buckling requires two types of analyses. The first type of analysis is known as Eigenvalue analysis that estimates the buckling modes. This is a linear elastic analysis performed using the (*BUCKLE) procedure available in ABAQUS

library with the load applied within the step. The lowest buckling mode predicted from the Eigenvalue analysis is used. The second type of analysis is called load-displacement nonlinear analysis and follows the Eigenvalue prediction. The ultimate loads, failure modes and axial shortenings as well as any other required data are determined from this analysis. The initial imperfections and material nonlinearity are included in the load-displacement analysis.

3.2. Finite element type and mesh

The 4-noded doubly curved shell elements with reduced integration S4R is used to model the buckling behaviour of cold-formed stainless steel circular hollow section columns. The S4R element has six degrees of freedom per node and provides accurate solution to most applications. The element accounts for finite strain and suitable for large strain analysis. In order to choose the finite element mesh that provides accurate results with minimum computational time, convergence studies were conducted. It is found that the mesh size around 10 mm × 10 mm (length by width) provides adequate accuracy and minimum computational time in modeling the cold-formed stainless steel circular hollow section columns.

3.3. Boundary conditions and load application

Following the testing procedures for Series C1, C2 and C3, the ends of the columns were fixed against all degrees of freedom except for the displacement at the loaded end in the direction of the applied load. The nodes other than the two ends were free to translate and rotate in any directions. The load was applied in increments using the modified RIKS method available in the ABAQUS library. The RIKS method is generally used to predict unstable and non-linear collapse of a structure. The load was applied as static uniform loads at each node of the loaded end using displacement control which is identical to the experimental investigation. The non-linear geometry parameter (*NLGEOM) was included to deal with the large displacement analysis.

3.4. Material modeling

The measured stress-strain curves of Series C1, C2 and C3 were used in the analysis. The static stress-strain curves were first obtained by knowing the static loads near the 0.2% proof stress and ultimate stress. The material behaviour provided by ABAQUS allows for a multi-linear stress-strain curve to be used. The first part of the multi-linear curve represents the elastic part up to the proportional limit stress with measured Young's modulus and Poisson's ratio was taken as 0.3. Since the analysis of post-buckling involves large in-elastic strains, the nominal (engineering) static stress-strain curve was converted to true stress and logarithmic plastic true strain curve. The true stress σ_{true} and plastic true strain ε_{true}^{pl} were calculated using Eqs. (1) and (2):

$$\sigma_{true} = \sigma(1 + \varepsilon) \quad (1)$$

$$\varepsilon_{true}^{pl} = \ln(1 + \varepsilon) - \sigma_{true} / E_0 \quad (2)$$

where E_0 is the initial Young's modulus, σ and ε are the measured nominal (engineering) stress and strain values, respectively.

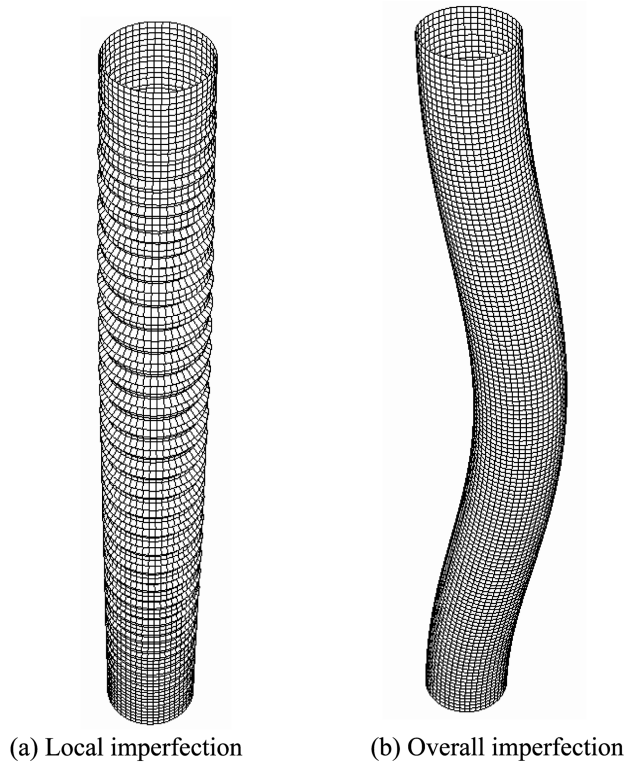


Fig. 4 Initial geometric imperfection modes (Eigenmode 1) for specimen C2L1500

3.5. Modeling of initial local and overall geometric imperfections

Cold-formed stainless steel columns with large D/t ratio are likely to fail by local buckling or interaction of local and overall buckling depending on the column length and dimension. Both initial local and overall geometric imperfections were found in the tested columns. Hence, superposition of local buckling mode as well as overall buckling mode with measured magnitudes is recommended in the finite element analysis. These buckling modes can be obtained by carrying Eigenvalue analyses of the column with large D/t ratio as well as small D/t ratio to ensure local and overall buckling occurs, respectively. Only the lowest buckling mode (Eigenmode 1) was used in the Eigenvalue analyses. This technique was used in this study to model the initial local and overall imperfections of the columns. Since all buckling modes predicted by ABAQUS Eigenvalue analysis are normalized to 1.0, the buckling modes were factored by the measured magnitudes of the initial local and overall geometric imperfections. Fig. 4 shows the local and overall imperfection buckling modes for specimen C2L1500.

3.6 Modeling of residual stresses

Previous studies by Gardner (2002) and Ellobody and Young (2005) on cold-formed stainless steel square and rectangular hollow section columns have shown that the effect of residual stresses on the column capacity is considered to be small. Cold-formed square and rectangular hollow sections are formed by cold-rolling with the weld of annealed flat strip into a circular hollow section, and then

further rolled into square or rectangular hollow section. Hence, the effect of residual stresses on the strength and behaviour of cold-formed stainless steel circular hollow section columns would be smaller than those of the square and rectangular hollow sections. Hence, residual stresses were not included in the finite element model.

4. Verification of finite element model

A total of 15 cold-formed stainless steel circular hollow section columns were used to verify the finite element model. The comparison of the ultimate loads (P_{Test} and P_{FE}) and axial shortening (e_{Test} and e_{FE}) at the ultimate loads obtained experimentally and numerically are shown in Table 1. It can be seen that good agreement has been achieved between both results for most of the columns. The column strengths obtained from the finite element analysis are slightly higher than that of the column test strengths with a maximum difference of 5% for C2L550 column. The mean value of P_{Test}/P_{FE} ratio is 0.98 with the corresponding coefficient of variation (COV) of 0.016, as shown in Table 1. The mean value of e_{Test}/e_{FE} ratio is 0.99 with the COV of 0.095. Three modes of failure have been observed experimentally and confirmed numerically by the finite element analysis. The failure modes were yielding failure (Y), local buckling (L) and flexural buckling (F).

Fig. 5 shows the applied load against the axial shortening behaviour of column specimen C3L1000 that has an outer diameter of 322.8 mm and a length of 1000 mm. The curve has been predicted using the finite element analysis and compared with the test curve. It can be seen that generally good

Table 1 Comparison between test and finite element results

| Specimen | Test | | FE | | | Test/FE | |
|----------|--------------------|--------------------|------------------|------------------|-----------------|---------------------------|---------------------------|
| | P_{Test} (kN) | e_{Test} (mm) | P_{FE} (kN) | e_{FE} (mm) | Failure mode | $\frac{P_{Test}}{P_{FE}}$ | $\frac{e_{Test}}{e_{FE}}$ |
| C1L550 | 235.2 | 16.88 | 240.5 | 15.41 | Y | 0.98 | 1.10 |
| C1L1000 | 198.4 | 10.26 | 206.8 | 10.89 | Y | 0.96 | 0.94 |
| C1L1500 | 177.4 | 5.77 | 181.8 | 6.54 | F | 0.98 | 0.88 |
| C1L2000 | 165.1 | 4.83 | 167.9 | 5.54 | F | 0.98 | 0.87 |
| C1L2500 | 151.6 | 5.39 | 148.9 | 5.93 | F | 1.02 | 0.91 |
| C1L3000 | 133.4 | 4.99 | 134.5 | 5.41 | F | 0.99 | 0.92 |
| C2L550 | 495.6 | 9.41 | 522.0 | 8.32 | Y | 0.95 | 1.13 |
| C2L1000 | 474.9 | 14.64 | 486.7 | 13.03 | L | 0.98 | 1.12 |
| C2L1500 | 461.0 | 15.92 | 468.9 | 15.25 | L + F | 0.98 | 1.04 |
| C2L2000 | 431.6 | 13.32 | 443.7 | 15.11 | L + F | 0.97 | 0.88 |
| C3L1000 | 1123.9 | 8.05 | 1140.0 | 7.93 | Y | 0.99 | 1.02 |
| C3L1500 | 1119.7 | 14.38 | 1130.0 | 13.12 | Y | 0.99 | 1.10 |
| C3L2000 | 1087.8 | 14.53 | 1100.0 | 14.90 | L | 0.99 | 0.98 |
| C3L2500 | 1045.7 | 19.12 | 1070.0 | 18.05 | L | 0.98 | 1.06 |
| C3L3000 | 1009.5 | 15.64 | 1040.0 | 16.74 | L | 0.97 | 0.93 |
| Mean | - | - | - | - | - | 0.98 | 0.99 |
| COV | - | - | - | - | - | 0.016 | 0.095 |

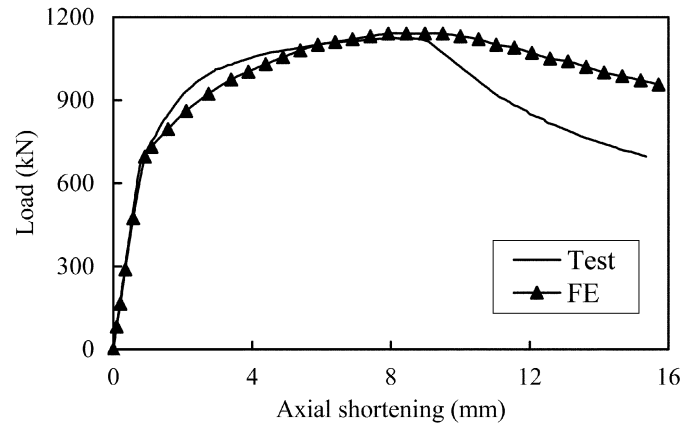
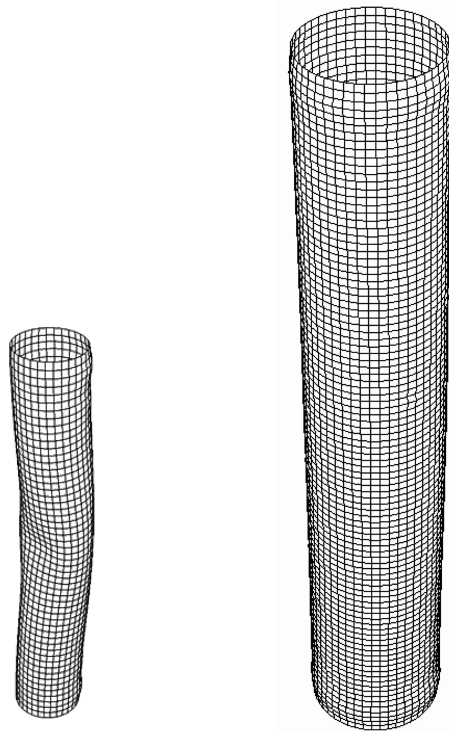


Fig. 5 Load-axial shortening curves for column C3L1000



(a) Specimen C1L550

(b) Specimen C2L1000

Fig. 6 Failure modes obtained from finite element analysis for specimens C1L550 and C2L1000

agreement between experimental and finite element results. The experimental ultimate load was 1123.9 kN with an axial shortening at the ultimate load of 8.05 mm compared with 1140.0 kN and 7.93 mm, respectively, predicted by the finite element analysis. Fig. 6 shows the failure modes of columns C1L550 and C2L1000 obtained from the finite element analysis. The failure mode of specimen C1L550 was yielding, while that of specimen C2L1000 was local buckling, as shown in Fig. 6.

5. Parametric study

The finite element (FE) model accurately predicted the behaviour of the cold-formed stainless steel circular hollow section columns. Therefore, parametric study was carried out to study the effect of local buckling on the strength and behaviour of the slender circular hollow section columns. A total of 42

Table 2 Specimen dimensions of the parametric study

| Specimen | D (mm) | t (mm) | D/t | L (mm) |
|-----------|----------|----------|-------|----------|
| C100L500 | 100 | 1.0 | 100 | 500 |
| C100L1000 | 100 | 1.0 | 100 | 1000 |
| C100L1500 | 100 | 1.0 | 100 | 1500 |
| C100L2000 | 100 | 1.0 | 100 | 2000 |
| C100L2500 | 100 | 1.0 | 100 | 2500 |
| C100L3000 | 100 | 1.0 | 100 | 3000 |
| C100L3500 | 100 | 1.0 | 100 | 3500 |
| C120L500 | 120 | 1.0 | 120 | 500 |
| C120L1000 | 120 | 1.0 | 120 | 1000 |
| C120L1500 | 120 | 1.0 | 120 | 1500 |
| C120L2000 | 120 | 1.0 | 120 | 2000 |
| C120L2500 | 120 | 1.0 | 120 | 2500 |
| C120L3000 | 120 | 1.0 | 120 | 3000 |
| C120L3500 | 120 | 1.0 | 120 | 3500 |
| C140L500 | 140 | 1.0 | 140 | 500 |
| C140L1000 | 140 | 1.0 | 140 | 1000 |
| C140L1500 | 140 | 1.0 | 140 | 1500 |
| C140L2000 | 140 | 1.0 | 140 | 2000 |
| C140L2500 | 140 | 1.0 | 140 | 2500 |
| C140L3000 | 140 | 1.0 | 140 | 3000 |
| C140L3500 | 140 | 1.0 | 140 | 3500 |
| C160L500 | 160 | 1.0 | 160 | 500 |
| C160L1000 | 160 | 1.0 | 160 | 1000 |
| C160L1500 | 160 | 1.0 | 160 | 1500 |
| C160L2000 | 160 | 1.0 | 160 | 2000 |
| C160L2500 | 160 | 1.0 | 160 | 2500 |
| C160L3000 | 160 | 1.0 | 160 | 3000 |
| C160L3500 | 160 | 1.0 | 160 | 3500 |
| C180L500 | 180 | 1.0 | 180 | 500 |
| C180L1000 | 180 | 1.0 | 180 | 1000 |
| C180L1500 | 180 | 1.0 | 180 | 1500 |
| C180L2000 | 180 | 1.0 | 180 | 2000 |
| C180L2500 | 180 | 1.0 | 180 | 2500 |
| C180L3000 | 180 | 1.0 | 180 | 3000 |
| C180L3500 | 180 | 1.0 | 180 | 3500 |
| C200L500 | 200 | 1.0 | 200 | 500 |
| C200L1000 | 200 | 1.0 | 200 | 1000 |
| C200L1500 | 200 | 1.0 | 200 | 1500 |
| C200L2000 | 200 | 1.0 | 200 | 2000 |
| C200L2500 | 200 | 1.0 | 200 | 2500 |
| C200L3000 | 200 | 1.0 | 200 | 3000 |
| C200L3500 | 200 | 1.0 | 200 | 3500 |

Table 3 Comparison of column strengths

| Specimen | P_{FE} (kN) | e_{FE} (mm) | Failure mode | $\frac{P_{FE}}{P_{ASCE}}$ | $\frac{P_{FE}}{P_{AS/NZS}}$ | $\frac{P_{FE}}{P_{EC3}}$ | $\frac{P_{FE}}{P_P}$ |
|-----------|------------------|------------------|-----------------|---------------------------|-----------------------------|--------------------------|----------------------|
| C100L500 | 91.8 | 4.70 | Y | 1.22 | 1.10 | 1.10 | 1.22 |
| C100L1000 | 88.6 | 7.70 | Y | 1.18 | 1.06 | 1.06 | 1.17 |
| C100L1500 | 81.2 | 8.17 | L + F | 1.08 | 0.97 | 0.97 | 1.08 |
| C100L2000 | 75.0 | 8.83 | L + F | 1.00 | 0.90 | 0.90 | 0.99 |
| C100L2500 | 65.4 | 6.56 | L + F | 0.92 | 0.85 | 0.80 | 0.88 |
| C100L3000 | 59.9 | 6.85 | L + F | 0.94 | 0.87 | 0.77 | 0.85 |
| C100L3500 | 55.7 | 6.55 | L + F | 0.96 | 0.89 | 0.76 | 0.84 |
| C120L500 | 105.7 | 3.97 | Y | 1.25 | 1.05 | 1.05 | 1.18 |
| C120L1000 | 105.1 | 7.05 | Y | 1.24 | 1.05 | 1.05 | 1.18 |
| C120L1500 | 99.6 | 8.30 | L + F | 1.18 | 0.99 | 0.99 | 1.12 |
| C120L2000 | 94.2 | 9.55 | L + F | 1.11 | 0.94 | 0.94 | 1.06 |
| C120L2500 | 88.0 | 9.40 | L + F | 1.04 | 0.88 | 0.88 | 0.99 |
| C120L3000 | 78.3 | 8.13 | L + F | 0.98 | 0.84 | 0.79 | 0.89 |
| C120L3500 | 73.3 | 8.07 | L + F | 1.01 | 0.87 | 0.78 | 0.87 |
| C140L500 | 119.7 | 3.24 | Y | 1.27 | 1.02 | 1.02 | 1.17 |
| C140L1000 | 119.5 | 6.23 | Y | 1.27 | 1.02 | 1.02 | 1.16 |
| C140L1500 | 116.1 | 8.05 | L | 1.24 | 0.99 | 0.99 | 1.13 |
| C140L2000 | 111.8 | 9.28 | L | 1.19 | 0.95 | 0.95 | 1.09 |
| C140L2500 | 106.6 | 9.98 | L + F | 1.13 | 0.91 | 0.91 | 1.04 |
| C140L3000 | 101.8 | 10.74 | L + F | 1.08 | 0.87 | 0.87 | 0.99 |
| C140L3500 | 91.7 | 9.64 | L + F | 1.04 | 0.85 | 0.80 | 0.91 |
| C160L500 | 134.2 | 3.10 | Y | 1.30 | 1.00 | 1.00 | 1.16 |
| C160L1000 | 134.1 | 5.95 | Y | 1.30 | 1.00 | 1.00 | 1.16 |
| C160L1500 | 132.4 | 7.97 | L | 1.28 | 0.99 | 0.99 | 1.14 |
| C160L2000 | 127.9 | 9.21 | L | 1.24 | 0.95 | 0.95 | 1.10 |
| C160L2500 | 124.8 | 10.49 | L + F | 1.21 | 0.93 | 0.93 | 1.08 |
| C160L3000 | 119.9 | 11.16 | L + F | 1.16 | 0.89 | 0.89 | 1.04 |
| C160L3500 | 114.1 | 11.35 | L + F | 1.10 | 0.85 | 0.85 | 0.99 |
| C180L500 | 147.5 | 2.83 | L | 1.31 | 0.98 | 0.98 | 1.15 |
| C180L1000 | 147.4 | 5.33 | L | 1.31 | 0.98 | 0.98 | 1.15 |
| C180L1500 | 147.3 | 7.58 | L | 1.31 | 0.98 | 0.98 | 1.14 |
| C180L2000 | 142.6 | 9.32 | L | 1.27 | 0.95 | 0.95 | 1.11 |
| C180L2500 | 140.6 | 10.32 | L | 1.25 | 0.93 | 0.93 | 1.09 |
| C180L3000 | 135.7 | 11.15 | L + F | 1.21 | 0.90 | 0.90 | 1.05 |
| C180L3500 | 132.0 | 11.46 | L + F | 1.17 | 0.88 | 0.88 | 1.03 |
| C200L500 | 157.9 | 2.18 | L | 1.30 | 0.94 | 0.94 | 1.12 |
| C200L1000 | 157.9 | 4.34 | L | 1.30 | 0.94 | 0.94 | 1.12 |
| C200L1500 | 157.9 | 6.50 | L | 1.30 | 0.94 | 0.94 | 1.12 |
| C200L2000 | 156.9 | 8.07 | L | 1.29 | 0.94 | 0.94 | 1.11 |
| C200L2500 | 155.3 | 9.75 | L | 1.28 | 0.93 | 0.93 | 1.10 |
| C200L3000 | 150.8 | 10.54 | L + F | 1.24 | 0.90 | 0.90 | 1.06 |
| C200L3500 | 147.7 | 11.64 | L + F | 1.21 | 0.88 | 0.88 | 1.04 |
| Mean | --- | --- | --- | 1.18 | 0.94 | 0.93 | 1.07 |
| COV | --- | --- | --- | 0.098 | 0.068 | 0.088 | 0.092 |

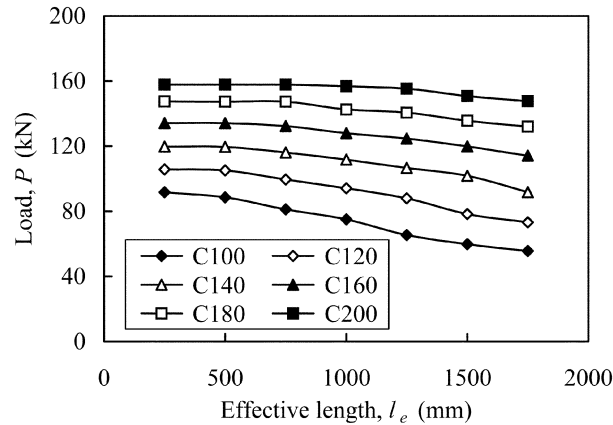


Fig. 7 Column strengths and effective length relationships obtained from parametric study

columns was performed in the parametric study. The columns are labeled such that the outer diameter and column length could be identified from the label. For example, the label “C100L1000” defines the circular hollow section column using a letter “C” followed by the value of the outer diameter in mm (100 mm) and the letter “L” indicates the length of the column followed by the column length in mm (1000 mm). Six series of slender circular hollow sections (Series C100, C120, C140, C160, C180 and C200) having the outer diameter of 100, 120, 140, 160, 180 and 200 mm, respectively, and a plate thickness of 1.0 mm were studied. The Series C100, C120, C140, C160, C180 and C200 had the outer diameter-to-thickness ratio (D/t) of 100, 120, 140, 160, 180 and 200, respectively. Each series of columns consists of seven column lengths of 500, 1000, 1500, 2000, 2500, 3000 and 3500 mm. A summary of the specimen dimensions of the parametric study is presented in Table 2. The maximum initial local geometric imperfection magnitude was taken as the measured value of Series C1 which is equal to 3.2% of the plate thickness. The initial overall geometric imperfection magnitude was taken as the average of the measured overall imperfections of the Series C1 which is equal to $L/1715$, where L is the column length. The measured stress-strain curve of Series C1 was used in the parametric study. A summary of the parametric study results is presented in Table 3. The ultimate loads (P_{FE}), axial shortening (e_{FE}) at the ultimate loads and failure modes are given in Table 3. The yielding failure mode (Y) was obtained for the columns of Series C100, C120, C140 and C160 with the lengths of 500 mm and 1000 mm. Interaction of local and flexural buckling (L + F) was predicted for columns of Series C100 and C120 with the lengths ranged from 1500 to 3500 mm and columns of Series C140 and C160 with the lengths varied from 2500 to 3500 mm as well as for columns of Series C180 and C200 with the lengths of 3000 and 3500 mm. The local buckling mode was predicted for the reminding of the columns in the parametric study. The ultimate loads obtained from the parametric study were also plotted against the effective length l_e ($l_e=L/2$) as shown in Fig. 7.

6. Design rules

6.1. General

The design rules specified in the ASCE Specification are based on the Euler column strength that requires the calculation of tangent modulus (E_t) using an iterative design procedure. The design rules

specified in the EC3 are based on the Perry curve that needs only the initial Young's modulus (E_o) and a number of parameters to calculate the design stress. The design rules specified in the AS/NZS Standard adopts either the Euler column strength or alternatively the Perry curve and the latter is used in this paper. The fixed ended columns were designed as concentrically loaded compression members and the effective length (l_e) was taken as one-half of the column length ($l_e = L/2$) as recommended by Young and Rasmussen (1998). In the three specifications, the effective area (A_e) is to account for local buckling of slender sections.

6.2. American Specification (ASCE)

The unfactored design strength for concentrically loaded cylindrical tubular compression members in the ASCE Specification (2002) is calculated as follows:

$$P_{ASCE} = F_n A_e \quad (3)$$

The flexural buckling stress (F_n) that account for overall buckling is calculated as follows:

$$F_n = \frac{\pi^2 E_t}{(l_e/r)^2} \leq F_y \quad (4)$$

where E_t is the tangent modulus determined using Eqn. (B-2) of the ASCE Specification, l_e is the effectively length, r is the radius of gyration of the full cross-section, and F_y is the yield stress that is equal to the static 0.2% proof stress ($\sigma_{0.2}$).

The effective area (A_e) that account for local buckling is calculated as follows:

$$A_e = \left[1 - \left(1 - \left(\frac{E_t}{E_o} \right)^2 \right) \left(1 - \frac{A_o}{A} \right) \right] A \quad (5)$$

where E_o is the initial Young's modulus, A is the full cross-section area, and A_o is the reduced cross-section area determined as follows:

$$A_o = K_c A \leq A \quad \text{for} \quad \frac{D}{t} \leq \frac{0.881 E_o}{F_y} \quad (6)$$

and

$$K_c = \frac{(1 - C)(E_o/F_y)}{(8.93 - \lambda_c)(D/t)} + \frac{5.882C}{8.93 - \lambda_c} \quad (7)$$

where C is the ratio of effective proportional limit-to-yield strength as given in Table A17 of the ASCE Specification, $\lambda_c = 3.084C$ with a limiting value of $(E_o/F_y)/(D/t)$, and D is the outer diameter and t is the plate thickness of the stainless steel tube.

6.3. Australian New/Zeland Standard (AS/NZS)

The unfactored design strength for concentrically loaded cylindrical tubular compression members in the AS/NZS Standard (2001) is calculated using the Perry curve as follows:

$$P_{AS/NZS} = F_n A_e \quad (8)$$

where

$$F_n = \frac{F_y}{\phi + \sqrt{\phi^2 - \lambda^2}} \leq F_y \quad (9)$$

$$\phi = 0.5(1 + \eta + \lambda^2) \quad (10)$$

$$\eta = \alpha((\lambda - \lambda_1)^\beta - \lambda_0) \geq 0 \quad (11)$$

$$\lambda = \frac{l_e}{r} \sqrt{\frac{F_y}{\pi^2 E_o}} \quad (12)$$

The parameters α , β , λ_0 and λ_1 required for the calculation of the AS/NZS design strengths were calculated from the equations proposed by Rasmussen and Rondal (1997) depending on the $(\sigma_{0.2}/E_o)$ ratio and the Ramberg-Osgood parameter (n) obtained from the tensile coupon of Series C1. The calculated values were 1.483, 0.231, 0.608 and 0.272 for the parameters α , β , λ_0 and λ_1 , respectively. The columns investigated in the parametric study had slenderness (λ) ranged from 0.043 to 0.06 calculated using Eq. (12), which covered the short to intermediate column slenderness. Hence, the results of the present study are limited to cold-formed stainless steel slender circular hollow sections for short to intermediate column slenderness. The effective area (A_e) is calculated in the same way as the ASCE Specification (2002), except for the reduction factor K_c as shown in Eq. (7). In the AS/NZS Standard, the reduction factor K_c is calculated as follows:

$$K_c = \frac{(1 - C)(E_o / F_y)}{(3.226 - \lambda_c)(D / t)} + \frac{0.178C}{3.226 - \lambda_c} \quad (13)$$

6.4. European Code (EC3)

The unfactored design strength for concentrically loaded cylindrical tubular compression members in the EC3 Code (1996) is calculated as follows:

$$P_{EC3} = \chi F_y A_e \quad (14)$$

where

$$\chi = \frac{1}{\phi + \sqrt{\phi^2 - \bar{\lambda}^2}} \leq 1 \quad (15)$$

$$\phi = 0.5(1 + \alpha(\bar{\lambda} - \bar{\lambda}_0) + \bar{\lambda}^2) \quad (16)$$

$$\bar{\lambda} = \frac{l_e}{r} \sqrt{\frac{F_y \beta_A}{\pi^2 E_o}} \quad (17)$$

$$\beta_A = \begin{cases} 1 & \text{for Class 1, 2 or 3 cross sections} \\ \frac{A_e}{A} & \text{for Class 4 cross sections} \end{cases} \quad (18)$$

The values of the imperfection factor α and limiting slenderness $\bar{\lambda}_o$ can be obtained from Table 5.2 of the EC3 Code.

The effective area (A_e) is taken as the full area (A) for Class 1 ($D/t \leq 50\varepsilon^2$), Class 2 ($D/t \leq 70\varepsilon^2$) and Class 3 ($D/t \leq 90\varepsilon^2$) cross-sections, where ε is calculated as follows:

$$\varepsilon = \sqrt{\frac{235}{F_y} \frac{E_o}{210000}} \quad (19)$$

It should be noted that the EC3 Code (1996) does not provide design rules for the calculation of effective area (A_e) for Class 4 ($D/t > 90\varepsilon^2$) slender circular hollow sections. In this study, the circular hollow sections investigated in the parametric study are classified as Class 4 slender sections, but no design provision is given in the EC3 Code for the calculation of the effective area. Hence, the full cross-section area (A) was used.

6.5. Proposed design equation

In this study, effective area equation for cold-formed stainless steel slender circular hollow section columns was proposed. The proposed effective area equation for Class 4 slender circular hollow sections is as follows:

$$A_e = A \varepsilon \left(\frac{125}{D/t} \right)^{0.1} \quad (20)$$

where A is the full cross-section area, ε is calculated from Eq. (19), D is the outer diameter and t is the plate thickness of the circular stainless steel tube.

The proposed design strength for concentrically loaded cylindrical tubular compression members can be calculated in the same way as the EC3 Code (1996):

$$P_p = \chi F_y A_e \quad (21)$$

where χ is the reduction factor for flexural buckling that is calculated in the same way as in Eq. (15), F_y is the yield stress that is equal to the static 0.2% proof stress ($\sigma_{0.2}$), and A_e is the proposed effective area as shown in Eq. (20).

6.6. Comparison of column strengths

The column strengths predicted from the parametric study were compared with the unfactored design strengths calculated using the American (ASCE 2002), Australian/New Zealand (AS/NZS 2001) and European (EC3 1996) specifications for cold-formed stainless steel structures. The measured material properties obtained from the tensile coupon of Series C1, which is the same material properties as those used in the parametric study, were used to calculate the design strengths. Table 3 shows the ratios of the

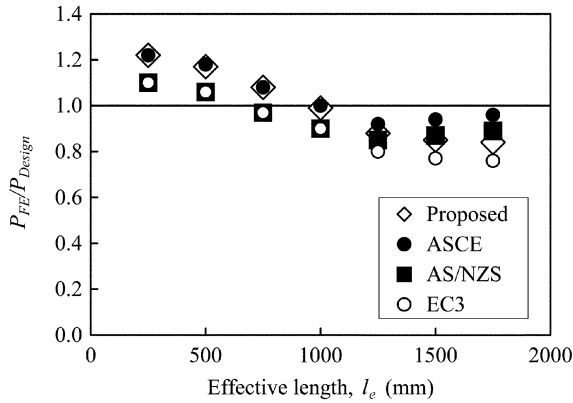


Fig. 8 Comparison of FE strengths with design strengths for Series C100

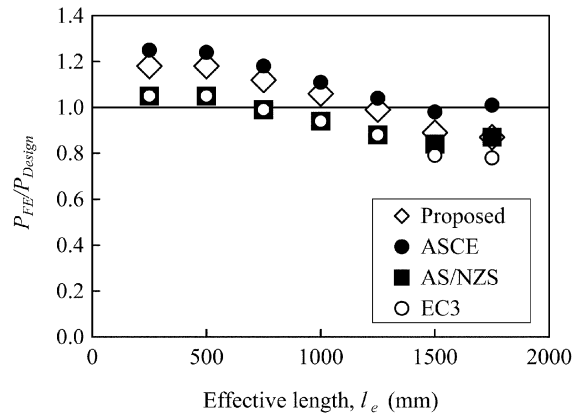


Fig. 9 Comparison of FE strengths with design strengths for Series C120

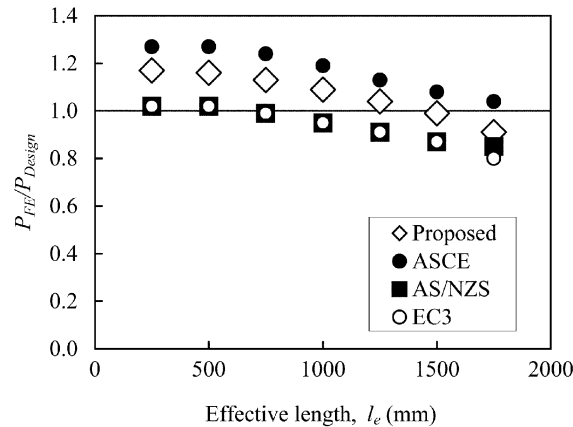


Fig. 10 Comparison of FE strengths with design strengths for Series C140

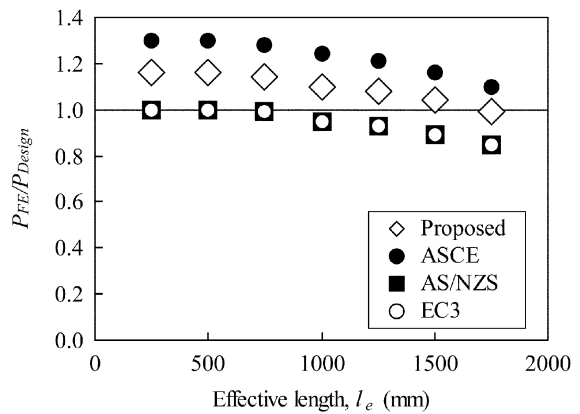


Fig. 11 Comparison of FE strengths with design strengths for Series C160

column strengths obtained from the finite element analysis and the design strengths (P_{FE}/P_{ASCE} , $P_{FE}/P_{AS/NZS}$, P_{FE}/P_{EC3} and P_{FE}/P_P). The mean values of P_{FE}/P_{ASCE} , $P_{FE}/P_{AS/NZS}$, P_{FE}/P_{EC3} and P_{FE}/P_P ratios are 1.18, 0.94, 0.93 and 1.07 with the corresponding coefficients of variation (COV) of 0.098, 0.068, 0.088 and 0.092, respectively. The column strength ratios for all specimens are shown on the vertical axis of Figs. 8-13, while the horizontal axis is plotted against the effective length (l_e) that is assumed equal to one-half of the column length. Figs. 8 and 9 show that the design strengths calculated using the AS/NZS and EC3 specifications are unconservative for the columns having D/t ratios of 100 and 120, except for the short columns with lengths of 500 and 1000 mm. The design strengths calculated using the American Specification and the proposed design equation are generally conservative, except for some long columns. Figs. 10-13 show that the design strengths calculated using the AS/NZS and EC3 specifications are generally unconservative for cold-formed stainless steel slender circular hollow section columns having D/t ratios of 140, 160, 180 and 200, while the ASCE Specification is quite conservative. The design strengths predicted using the proposed design equation are generally conservative for cold-formed stainless steel slender circular hollow section columns having D/t ratios of 140, 160, 180 and 200.

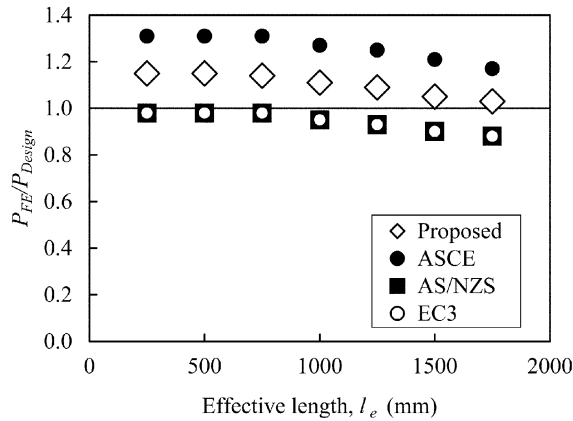


Fig. 12 Comparison of FE strengths with design strengths for Series C180

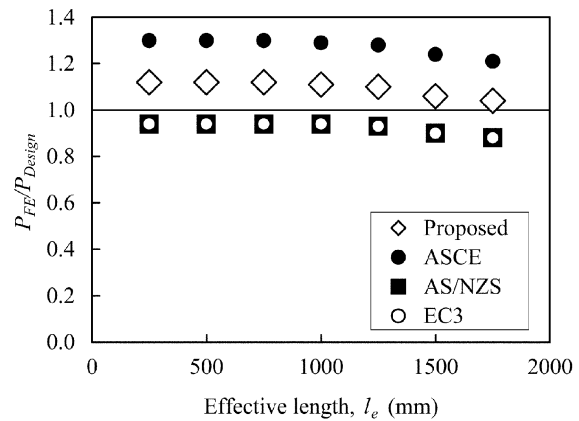


Fig. 13 Comparison of FE strengths with design strengths for Series C200

7. Conclusions

The behaviour of cold-formed stainless steel slender circular hollow sections with large diameter-to-plate thickness (D/t) ratio has been investigated. An accurate nonlinear finite element model for the analysis of the stainless steel slender circular hollow section columns was presented. The material nonlinearity and geometric imperfections of the columns have been considered in the finite element model. The results obtained from the finite element analysis were compared well with the experimental results. Therefore, parametric study of cold-formed stainless steel slender circular hollow section columns with large D/t ratio ranged from 100 to 200 for short to intermediate column slenderness was performed using the finite element model.

The results of the parametric study have shown that the design rules specified in the Australian/New Zealand and European specifications are generally unconservative for the cold-formed stainless steel slender circular hollow section columns with large D/t ratio, while the American Specification is generally quite conservative. It should be noted that the European Code does not provide design rules for the calculation of effective area for slender circular hollow sections, hence, the full cross-section area was used. Design equation was proposed to evaluate the axial strength of cold-formed stainless steel slender circular hollow section columns. The design strengths predicted using the proposed equation are generally more accurate compared with the design strengths calculated using the American, Australian/New Zealand and European specifications.

References

- ABAQUS Standard User's Manual. (2004), Hibbit, Karlsson and Sorensen, Inc. Vol. 1, 2 and 3, Version 6.4, USA.
- ASCE (2002), *Specification for the design of cold-formed stainless steel structural members*. American Society of Civil Engineers, SEI/ASCE-8-02, Reston, Virginia.
- AS (1991), *Methods for tensile testing of metals*. Australian Standard, AS 1391 – 1991, Standards Association of Australia, Sydney, Australia.

- AS/NZS (2001), *Cold-formed stainless steel structures*. Australian/New Zealand Standard, AS/NZS 4673:2001, Standards Australia, Sydney, Australia.
- EC3 (1996), *Eurocode 3: Design of steel structures – Part 1.4: General rules – Supplementary rules for stainless steels*. European Committee for Standardization, ENV 1993-1-4, CEN, Brussels.
- Ellobody, E. and Young, B. (2005), “Structural performance of cold-formed high strength stainless steel columns”, *J. Construct. Steel Res.*, **61**(12), 1631-1649.
- Gardner, L. (2002), “A new approach to structural stainless steel design”, PhD Thesis, Department of Civil and Environmental Engineering, Imperial College of Science, Technology and Medicine, London.
- Gardner, L. and Nethercot, D. A. (2004), “Numerical modeling of stainless steel structural components - A consistent approach”, *J. Struct. Eng.*, ASCE, **130**(10), 1586-1601.
- Jiao, H. and Zhao, X. L. (2003), “Imperfection, residual stress and yield slenderness limit of very high strength (VHS) circular steel tubes”, *J. Construct. Steel Res.*, **59**, 233-249.
- Macdonald, M., Rhodes, J. and Taylor, G. T. (2000), “Mechanical properties of stainless steel lipped channels”, *Proc. of the Fifteenth Int. Specialty Conf. on Cold-formed Steel Structures*, Eds R. A. LaBoube and W. W. Yu, St. Louis, University of Missouri-Rolla, Mo., USA, 673-686.
- Ramberg, W. and Osgood, W. R. (1943), “Description of stress strain curves by three parameters”, Tech. Note No 902, National Advisory committee for Aeronautics, Washington, D.C.
- Rasmussen, K. J. R. (2000), “Recent research on stainless steel tubular structures”, *J. Construct. Steel Res.*, **54**, 75-88.
- Rasmussen, K. J. R. and Hancock, G. J. (1993), “Design of cold-formed stainless steel tubular members. I: Columns”, *J. Struct. Eng.*, ASCE, **119**(8), 2349-2367.
- Rasmussen, K. J. R. and Rondal, J. (1997), “Strength curves for metal columns”, *J. Struct. Eng.*, ASCE, **113**(6), 721-728.
- Talja, A. and Salmi, P. (1995), “Design of stainless steel RHS beams, columns and beam-columns”, VTT Research Notes 1619, Technical Research Centre of Finland, Espoo.
- Young, B. (2005), “Local buckling and shift of effective centroid of cold-formed steel columns”, *Steel and Composite Structures*, **5**(2-3), 235-246.
- Young, B. and Hartono, W. (2002), “Compression tests of stainless steel tubular members”, *J. Struct. Eng.*, ASCE, **128**(6), 754-761.
- Young, B. and Liu, Y. (2003), “Experimental investigation of cold-formed stainless steel columns”, *J. Struct. Eng.*, ASCE, **129**(2), 169-176.
- Young, B. and Lui, W. M. (2005), “Behavior of cold-formed high strength stainless steel sections”, *J. Struct. Eng.*, ASCE, **131**(11), 1738-1745.
- Young, B. and Rasmussen, K. J. R. (1998), “Tests of fixed-ended plain channel columns”, *J. Struct. Eng.*, ASCE, **124**(2), 131-139.
- Young, B. and Rasmussen, K. J. R. (1999), “Shift of effective centroid of channel columns”, *J. Struct. Eng.*, ASCE, **125**(5), 524-531.

Notation

The following symbols are used in this paper

| | |
|---------------------------|---|
| A | : gross or full cross-section area |
| A_e | : effective cross-section area |
| A_o | : reduced cross-section area |
| C | : ratio of effective proportional limit-to-yield strength |
| D | : outer diameter |
| E_o | : initial Young's modulus |
| E_t | : tangent modulus |
| e_{FE} | : axial shortening from finite element analysis at failure |
| e_{Test} | : axial shortening from tests at failure |
| F_n | : flexural buckling stress |
| F_y | : yield stress ($F_y = \sigma_{0.2}$) |
| K_c | : reduction factor due to local buckling |
| L | : length of column specimen |
| l_e | : column effective length |
| n | : Ramberg-Osgood parameter |
| P | : axial compressive load |
| P_{ASCE} | : unfactored design strength of the American Specification |
| P_{ASNZS} | : unfactored design strength of the Australian/New Zealand Standard |
| P_{Design} | : unfactored design strength |
| P_{EC3} | : unfactored design strength of the European Code |
| P_{FE} | : finite element ultimate load |
| P_P | : unfactored design strength calculated using the proposed equation |
| P_{Test} | : test ultimate load |
| r | : radius of gyration |
| t | : plate thickness of specimen |
| α | : parameter used to define imperfection |
| β | : parameter used to define imperfection |
| χ | : reduction factor for flexural buckling |
| ε | : strain |
| ε_{true}^{pl} | : plastic true strain |
| λ_o | : parameter used to define imperfection |
| $\bar{\lambda}_o$ | : limiting slenderness for flexural buckling |
| λ_1 | : parameter used to define imperfection |
| σ | : stress |
| $\sigma_{0.2}$ | : static 0.2% tensile proof stress; and |
| σ_{true} | : true stress |

DN